Dalton Transactions

RSC Publishing

PAPER

View Article Online
View Journal | View Issue

Cite this: *Dalton Trans.*, 2013, **42**, 10898

Dinuclear complexes of copper and zinc with *m*-xylene/cyclohexane-linked bis-aspartic acids: Synthesis, characterization, dioxygen activation, and catalytic oxidation of nitrobenzene in pure aqueous solution†

Shourong Zhu,*[a] Zhixiang Qiu,[a] Tianjun Ni,*[b] Xiujuan Zhao,[a] Shikai Yan,[c] Feifei Xing,[a] Yongmei Zhao,[a] Yueling Bai[a] and Mingxing Li[a]

Received 8th April 2013,
Accepted 17th May 2013

DOI: 10.1039/c3dt50923k

www.rsc.org/dalton

Two new *m*-xylene/cyclohexane-linked bis-aspartic acid ligands, L_b and L_c, were synthesized *via* Michael addition in basic aqueous solution. Their structures were characterized by elemental analysis, NMR and MS spectrometry. Both ligands react with Cu(II) and Zn(II) to form dinuclear complexes, with $M_2L(OH)^-$ the major species in neutral/weak basic aqueous solution. To quantify the relative interaction strength between a Lewis acid and base, a new parameter $\sigma = \log K/14$ was proposed which compares the stability constant with the binding constant between H^+ and OH^-. The dinuclear copper complexes (L_b–2Cu and L_c–2Cu) react with H_2O_2 in aqueous solution. The reaction in 0.020 M phosphate buffer at pH 7.5 is first-order for [L_c–2Cu], but second-order for [L_b–2Cu]. The oxidation products are oxygenated and/or dehydrogenated species. Radical trapping tests indicate that both complexes slightly scavenge the $OH^{\cdot}$ radical, but generate the $H^{\cdot}$ radical. L_c–2Cu generates the $H^{\cdot}$ radical much more effectively than that of L_b–2Cu when reacted with H_2O_2. Both complexes are excellent catalysts for the oxidation of nitrobenzene in the presence of H_2O_2 in weakly basic aqueous solution. The oxidation follows the rate-law $v = k$[complex][nitrobenzene][H_2O_2]. The k values in pH 8.0 phosphate buffer at 25 °C are 211.2 ± 0.3 and 607.9 ± 1.7 $mol^{-2}\ L^2\ s^{-1}$ for L_b–2Cu and L_c–2Cu, respectively. The Arrhenius activation energies are 69.4 ± 2.2 and 70.0 ± 4.3 kJ mol^{-1} for L_b–2Cu and L_c–2Cu, respectively, while the Arrhenius pre-exponential factors are 2.62×10^{14} and 1.06×10^{15}, respectively. The larger pre-exponential factor makes L_c–2Cu more catalytically active than L_b–2Cu. These complexes are some of the most effective oxidation catalysts known for the oxidation of nitrobenzene.

1. Introduction

The synthesis of amino acids is of great importance. Non-proteinogenic α-amino acids are important in biological, medicinal and synthetic chemical applications.[1] The most effective carbon–nitrogen bond formation is by simple addition of amines to carbon–carbon double bonds.[2] Although the Mannich reaction is an effective method to form C–N bonds, Michael addition is a common approach for the synthesis of amino acids and their derivatives with 100% atom efficiency and without any byproduct formation.[3] The direct addition of amines to inactivated alkenes is very difficult to accomplish,[4] although the direct amination of α,β-unsaturated carboxylic acids can readily be effected.[5] Amination of unsaturated dicarboxylic acids, such as maleic and fumaric acid, is most successfully performed by aspartase enzymes.[6] However, there is no general one-step method for the synthesis of N-substituted

[a]*Department of Chemistry, College of Sciences, Shanghai University, Shanghai 200444, China. E-mail: shourongzhu@shu.edu.cn; Fax: +86-21-60947570; Tel: +86-21-66132403*
[b]*Department of Chemistry, Xinxiang Medical University, East of Jinsui Road, Xinxiang, Henan 453003, China*
[c]*School of Pharmacy, Shanghai Jiao Tong University, Shanghai 200240, China*

†Electronic supplementary information (ESI) available: Synthetic procedure of ligand L_b and L_c. IR spectra of ligand L_b and L_c. NMR of L_b and L_c in D_2O. EI-MS spectra of L_c and L_c in aqueous solution. pH titration curve of 1.000×10^{-3} M Cu_2-L_c in absence and presence of 10.00 eq. H_2O_2 at 25.0 ± 0.1 °C, I = 0.10 M KNO_3. Time dependences of 400 nm absorbance for the reaction of nitrobenzene and H_2O_2 in the presence of dinuclear copper complexes. Plot of the observed second-order rate constants determined at 360 nm as a function of [H_2O_2] for L_c-2Cu complexes. Radical scavenging spectra. Positive mass spectra of dinuclear copper complexes. X-band EPR spectra of 2.5×10^{-3} M copper(II) complex in the absence and presence of 80 equivalent H_2O_2 at different pH at −60 °C. First-order and second-order rate constants. See DOI: 10.1039/c3dt50923k

functionalized aspartic acids had been reported until 2005.[5] While aspartic acid synthesis in the presence of aspartate ammonia lyase,[7] and the conjugate addition of *N*-nucleophiles to substituted fumaric acids using methylaspartase are enantiospecific,[8] chemical addition of amine to C=C bond will generate racemic products.[8,9] Therefore, development of less expensive, simpler, "greener" methods for the reactions is still highly desirable. Liang *et al*. showed that the K_2CO_3 supported catalysts were very efficient for the reactions, but the product was racemic.[2] The enantioselective synthesis of amino acids is of great interest and there is no precedence for the synthesis of bis-aspartic acids.

Our goal is to synthesis bis-aspartic acids ligand that can form dinuclear complexes to investigate their dioxygen activation and catalytic oxidation. Oxidative transformations use dioxygen or H_2O_2 as an inexpensive, environmentally friendly oxidant in contrast to toxic chemical oxidants, and they exceed their chemical equivalent in regiospecificity and enantioselectivity.[10] The development of transition metal complexes as effective catalysts for a wide range of oxidative transformation reactions and the understanding of the latter processes still represent a fundamental challenge to inorganic chemists.[11] Inspired by biological systems, and in consideration of environmental aspects, the complexes of choice contain an iron, copper or manganese active site.[12] Although there are a large number of papers published on dioxygen activation or catalytic oxidation,[13] greener amino acid complexes for use as catalysts in these reactions are still scare. Recently, chloromethylated polystyrene supported alanine-dihydroxylbenzaldehyde Schiff base and 1,10-phenanthroline metal complexes for the oxidation of cumene by molecular oxygen have been reported.[14] Catalytic oxidation of substrates with Mn,[16] Ru, and Cu[17] amino acid complexes have also been reported. The most relevant study with respect to the work presented herein is the *enantio*-differentiating catalytic oxidation of reactive L- and D-dihydroxyphenylalanine (Dopa) by a biomimetic trinuclear copper complex containing two L-histidine residues. This reaction depends on the anchoring of the substrate provided by the third copper center which does not participate in the catalytic reaction and which recognizes the chirality of the substrate.[15]

We chose nitrobenzene as an organic substrate because nitrobenzene is an environmental pollutant which is quite difficult to oxidize. Nitrobenzene oxidation has been studied by Lu *et al. via* the Fenton reaction and other techniques.[16] Some other green oxidation catalysts have been reported,[17] such as a Mn-complex which catalyzed the oxidation of organic substrates in the presence of H_2O_2.[18] However, metal complex catalyzed oxidation of nitrobenzene is rare. One requirement for catalytic oxidation of an organic substrate is dioxygen activation, and complexes of dinuclear copper[19] or iron[20] are the most popular. Binuclear complexes, where the two tridentate donor groups are separated by an *m*-xylyl bridge, are somewhat similar to the active center of hemerythrin and hemocyanin. In 1984, Karlin *et al.* reported dioxygen activation by a bis(2-pyridylmethyl) amine substituted xylene copper(I) complex and found the product was xylyl hydroxylation.[21] Some similar results were reported later,[21,22] and ligand hydroxylation was also found to occur in iminodiacetate substituted analogs.[23] Ligand structure has a subtle influence on the dioxygen activation of their complexes. For example, *m*-xylyl bridged bis-iminodiacetate iron complex can activate dioxygen, but *m*-xylyl bridged bis(2-pyridylmethyl) amine iron complex cannot.[23] Most of the dioxygen activation studies are in non-aqueous solution at low temperature. Aqueous solution dioxygen activation is more desirable for practical usage, but on the whole, there are few reports of dioxygen activation in 100% aqueous solution. In this paper, we present a facile one-step, aqueous method for the preparation of N-substituted, functionalized bis-aspartic acids, pH titration studies of the ligands and their copper(II) and zinc(II) complexes, dioxygen activation by the complexes and catalytic oxidation of nitrobenzene substrates in the presence of H_2O_2 in aqueous solution.

2. Experimental section

Materials and methods

All chemicals were of reagent-grade quality, obtained from commercial sources and were used as received without further purification. Elemental analyses were determined using a Vario EL III elemental analyzer. The IR spectra were recorded in the 4000–400 cm^{-1} region using KBr pellets and a Nicolet AVATAR-370 spectrometer. NMR spectra were recorded on a BRUKER AV 500 MHz spectrometer. UV-vis spectra were recorded on a Puxi general TU-1900. Optical rotations were measured on Rudolph Research Analytical Autopol IV-T polarimeter.

ESI-MS analysis

ESI-MS analysis was performed on an Agilent-1100 HPLC system with a LC/MSD Trap XCT mass spectrometer (Agilent Corporation, MA, USA). The ESI-MS spectra were acquired in both positive and negative ion mode with the following conditions: drying gas N_2 at 10 L min^{-1}; temperature 350 °C; pressure of nebulizer 30 psi; capillary voltage 2500 V. Analyses were performed in the full scan mode (50–1500 *m*/*z*) with auto fragmentation. Data acquisition was performed using Chemstation software (Agilent Techniques, MA, USA).

HPLC-MS was measured on a Shimadzu LC-MS 2020 instrument with a C_{18} column at 25 °C, eluted with 70% methanol–30% H_2O. Column temperature was 40 °C. To 2.0 mL of L_b–2Cu or L_c–2Cu (pH 9.5) was added 20 μL of 30% H_2O_2, and the mixture was stirred for 1 h. K_2S solution (0.08 M, 50 μL) was added to the solution. The mixture was left at room temperature for half an hour and centrifuged to remove CuS.

Radical formation/scavenging test

Two methods were used to scavenge radicals. (a) 1,1-Diphenyl-2-picrylhydrazyl (DPPH) free radical scavenging activity assay:[24] dicopper(II) complex (L_b or L_c), dissolved in deionized water

(2 mL), was mixed with 2 mL of methanolic solution containing DPPH radicals, resulting in a final concentration of 1.00×10^{-4} M DPPH and 1.67×10^{-4} M copper(II) complex. The mixture was shaken vigorously and left to stand for 30 min in the dark, and the absorbance was then measured at 545 nm against a blank. The percentage of released radical was calculated as a formation ratio = $\{[1 - (A_1 - A_2)/A_0]\} \times 100\%$ where A_0 was the absorbance of the control (without copper complex), A_1 was the absorbance in the presence of the complex, and A_2 was the absorbance without DPPH. (b) $OH^{\cdot}$ scavenging assay: $OH^{\cdot}$ scavenger ability was measured according to a literature procedure.[24c] $OH^{\cdot}$ radicals were generated from $FeSO_4$ and H_2O_2, and detected by their ability to hydroxylate salicylate. The reaction mixture (3 mL) contained 1 mL $FeSO_4$ (1.5 mM), 0.7 mL H_2O_2 (6 mM), 0.3 mL sodium salicylate (20 mM) and 1.0 mL 2.5×10^{-4} M L_b–2Cu or L_c–2Cu. The absorption spectra were measured immediately and after 30 min at 25 °C. The percentage of radical released was calculated (500 nm absorption) in the same way as the DPPH method.

Reaction with H_2O_2 in aqueous solution

To a 2.00 mL of 0.050 M KH_2PO_4–NaOH solution at specific pH was added 2.00 mL of water, 1.00 mL of 2.5×10^{-3} M L_b–2Cu or L_c–2Cu aqueous solution. The pH was adjusted to 7.50 with 1.0 M NaOH or HNO_3. The final concentration of Cu complex was 5.00×10^{-4} M and the H_2O_2 concentrations varied from 0.10 to 0.50 M. The solution (2.0 mL) was equilibrated in a 1.00 cm cell at 25.0 ± 0.1 °C for 10 min. The required amount (20–80 μL) of 30% H_2O_2 was added to the solution, and absorbance of the solution was measured at 360 nm with 0.020 M buffer solution as a reference.

Catalytic oxidation

Nitrobenzene (6.0 μL) was dissolved in 40 mL of 0.2 M of KH_2PO_4–NaOH buffer (pH = 8.00) with stirring to give a 1.47×10^{-3} M nitrobenzene solution. The nitrobenzene solution (3.0 mL) was placed in a 1.0 cm quartz cell and thermally equilibrated at 25 °C for 5 min. Various amounts of L_b–2Cu or L_c–2Cu and H_2O_2 (30%) were added to the solution. The total volume was 3.0–3.1 mL. Reaction kinetics were monitored at 400 nm with buffer as the reference.

pH titration

The stability constants of the binary complexes were determined by pH-metric titrations on a Metrohm Titrando 809 equipped with a 800 Dosino and 6.0263.100 pH electrode. The samples contained either $Cu(NO_3)_2$ or $Zn(NO_3)_2$ and a ligand in a 2 : 1 mole ratio. The titration sample was 1.000×10^{-3} M in ligand. Pure, moist N_2(g) was bubbled through the sample to ensure the absence of O_2(g) and CO_2(g) and to stir the solutions. All pH titrations were carried out with 20 mL samples at 298.0 ± 0.1 K and a constant ionic strength of 0.10 M $NaNO_3$. Carbonate-free NaOH was used for all titrations as described previously.[25] The pH meter was calibrated at 4.003 (0.050 mol L^{-1} potassium hydrogen phthalate), 6.864 (0.025 mol L^{-1} Na_2HPO_4 and 0.025 mol L^{-1} KH_2PO_4 mixture) and 9.322 (0.010 mol L^{-1} disodium tetraborate), respectively. All pH titration experiments were run at least in duplicate to ensure reliability of the data. Data were acquired with TIMAO software. Ligand titrations were performed in the pH range ~2.5–12 and titrations on complexes in the pH range 3–11. Titration data were fitted with the program SCMAR (Newton–Gauss nonlinear least-squares).[26] The activity coefficient of H^+ and OH^- were taken from literature.[27]

Synthesis of L_b

To 10.0 g (0.10 mol) of maleic anhydride suspended in 30 mL water was slowly added 0.20 mol NaOH (in 5 mL water) at 75–85 °C to dissolve the maleic anhydride. 1,3-Xylenediamine (6.47 mL, 6.81 g, 50 mmol) was added to the solution. The mixture was refluxed for 3 days and the color changed from colorless to yellow–green. Maleic anhydride, disodium salt (5 g) was added to the solution, and the mixture was refluxed for an additional 2 days. The mixture was cooled to room temperature and filtered. To the filtrate was added a solution of 16.65 g (0.15 mol) of $CaCl_2$ in 20 mL water and the mixture was stirred overnight at room temperature. The newly precipitated solid was isolated by filtration and washed with water and ethanol to yield the calcium salt of the ligand L_b (20.84 g). To the calcium salt was added 100 mL of water and 0.15 mol $H_2C_2O_4$, and the mixture was stirred overnight. The CaC_2O_4 that formed was removed by filtration and the remaining solution was concentrated to 10 mL under reduced pressure. Acetone (~50 mL) was added to the residue and two layers were obtained. The upper acetone layer was discarded and the bottom layer (oil) was washed several times with 10 mL of ethanol. The oil was vacuum dried at 80 °C. It contained considerable water and foamed during vacuum drying. This compound was very hygroscopic. Yield 65%. Mp. 267–269 °C. IR ν_{max} 3429, 3020, 2825, 1722, 1626, 1406, 1221, 1057, 876, 706, 638 and 526 cm^{-1}; ^1H NMR (500 MHz, D_2O) δ 7.45 (s, 4H, aromatic proton), 4.25 (q, J = 13 Hz, 4H, Ar-CH2-), 3.90 (t, J = 2.8 Hz, 2H, N-CH), 2.90 (s, 4H, CH_2COO). α_D(18.5C) = 21.54. Elemental analysis found (calculated) for $Ca_{0.5}C_{16}H_{19}N_2O_8 \cdot 0.2H_2O$: C 49.38 (49.16); H 5.15 (5.00); N 6.92 (7.16).

Synthesis of L_c

To a 50 mL round bottom flask was added maleic anhydride (1.0 g, 10 mmol) and 10 mL water. The mixture was warmed to 75–85 °C and 2.0 mL of 10 M NaOH (20 mmol) was added. 1,3-Bis(aminomethyl)cyclohexane 0.71 g (5.0 mmol) was added and the solution was stirred for 3 days. The color gradually changed to light yellow. To make full use of the 1,3-bis(aminomethyl)cyclohexane, another 5 mmol of disodium maleate was added. After stirring the mixture for 2 days, the color became deep yellow. The solution was filtered and to the filtrate was added $CaCl_2$ (1.6 g, 15 mmol) in 5 mL of water. The mixture was stirred for 4 h, after which the white precipitate of the calcium salt of the ligand and any unreacted calcium maleate were removed by filtration. The solid was suspended in 10 mL water containing $H_2C_2O_4$ (1.83 g, 15 mmol) and stirred for 5 h.

The CaC_2O_4 was removed by filtration and washed with water. The aqueous solution was concentrated to 2 mL under reduced pressure, and acetone was added to give two layers. The upper acetone layer was discarded to remove $H_2C_2O_4$ and maleic acid. The bottom layer was washed with ethanol until it was colorless. The oil was vacuum dried at 80 °C. Pure L_c was obtained in ~60% yield. IR (cm^{-1}): 3429, 2929, 2856, 1716, 1629, 1389, 1081, 1043, 871, 652 and 546. ^{13}C NMR (500 MHz, D_2O): 176, 172, 58, 52, 34.5, 34, 33, 28, 24. MS (ESI) calcd for $C_{16}H_{26}N_2O_8$ $(M + H)^+$, 375, found 375. α_D(18.5C) = 152.4. Elemental analysis found (calculated) for $Ca_{0.5}(C_{16}H_{25}N_2O_8)\cdot 3.5H_2O$ (FW = 456.4): C, 41.95 (42.10); H, 6.92 (7.06); N, 6.39 (6.13).

3. Results and discussion

Synthesis of ligands

Reports of bis-aspartic acids are quite rare[28] except for some patents.[29] We chose flexible diamines, namely, 1,3-cyclohexanedimethanamine and 1,3-benzenedimethanamine to react with inexpensive maleic anhydride in basic aqueous solution for the synthesis of *N*,*N*′-(*m*-phenylenedimethylene) bis-aspartic acid and *N*,*N*′-(1,3-cyclohexanedimethylene) bis-aspartic acid, respectively (Scheme 1). Although L_b has been mentioned in patents,[30] and Kezerian also mentioned this compound in a report,[31] no synthetic details were provided. However, the reaction of primary amines with electron-deficient alkenes has been studied by several authors.[2,32] Due to their highly hydrophilic properties and very poor solubility in organic solvents, we encountered great difficulty in the purification of the products, but we found that the bis-aspartic acids formed calcium salts that were insoluble in aqueous solution. Removal of the Ca as CaC_2O_4 resulted in the acid form of the products. However, the acid form of the bis-aspartate was so hydrophilic

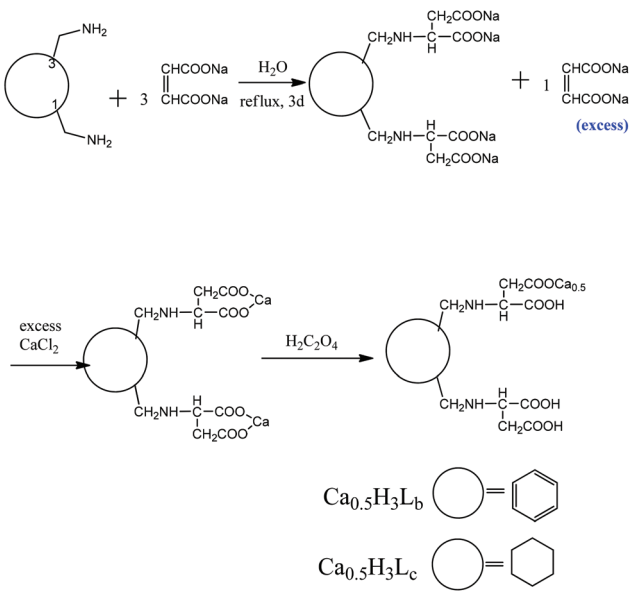

Scheme 1 Synthetic procedure of the ligands.

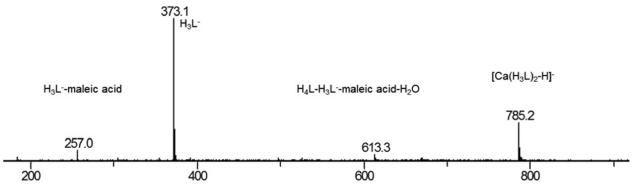

Fig. 1 ESI-MS spectrum of ligand L_c in the negative ion mode.

that concentration to a very small volume resulted in a colorless viscous oil, which still contained $H_2C_2O_4$. This was removed by washing with acetone. $H_2C_2O_4$ is a strong acid compared to aspartic acid, its pK_{a1} and pK_{a2} are 1.25 and 3.81 respectively. Theoretically, excess $H_2C_2O_4$ can fully protonate aspartate to form neutral aspartic acid. Beyond our expectation, from elemental analysis and pH titration, there were still calcium ions associated with the ligands; both of the bis-aspartic acids contained 0.5 calcium ion per molecule. The purity of *N*,*N*′-(*m*-phenylenedimethylene)bis-aspartic acid (L_b) was confirmed by a very clean ^1H NMR spectrum in D_2O solution (Fig. s2†). However, *N*,*N*′-(1,3-cyclohexanedimethylene) bis-aspartic acid (L_c) had a very complicated ^1H NMR in D_2O solution, possibly due to the presence of four chiral carbon atoms in L_c. To further clarify the composition, ESI-MS was used. L_c produced a very clean spectrum (Fig. 1).

From the MS spectrum, the parent ion peak, $H_3L_c^-$ (M^-) was located at 373.1, which is similar to the calculated value of 373.16. Its isotope pattern was also identical to the theoretical simulation. The second strong peak at 785.2 is $[Ca(H_3L_c)_2 - H^+]^-$. Positive spectra also coincided well with the structure (Fig. s5 and s6 in ESI†). Both ligands have optical rotation, which indicate both ligands are not a racemic mixture.

pH titration

Data for the titration of 1.00×10^{-3} M ligand in the absence and presence of 2 eq. $Zn(NO_3)_2$ or $Cu(NO_3)_2$ in I = 0.10 M KNO_3 are presented in Fig. 2. Computer simulation was used to obtain the ligand protonation constants and complex stabilities, which are summarized in Table 1. Although there is 0.5 Ca^{2+}, the interactions of Ca^{2+}, as well as Na^+ and K^+, with ligands are omitted.

From the titration curves (Fig. 2), both L_b and L_c exhibit pH jumps at H_2L^{2-}. This indicates that the last two protons dissociate at a much higher pH than the others. The titration curve of L_b is below that of L_c at pH 7 or higher, which means that the protonation constant of L_c is higher than that of L_b. Table 1 lists the cumulative protonation constants of L_b and L_c at 25 °C, I = 0.10 M KNO_3. Aspartic acid has three deprotonation processes; its stepwise protonation constants are pK_{a1} = 9.66, pK_{a2} = 3.71, pK_{a3} = 1.95.[33] Sajadi recently reported 9.90, 3.72 and 1.99 respectively at 25 °C.[34] Our data indicate that the bis-aspartic acids have six protonation processes. The K_{a1} and K_{a2} correspond to the first pK_a of the two aspartic acids in the ligand. They are 10.28 and 8.82 for L_b and 10.54 and 9.84 for L_c. The pK_{a1} of L_b and L_c are obviously larger than that of free aspartic acid. When statistical factors (concentration effect, 0.3

difference in pK_a) are taken into account, the pK_{a1} of L_b is comparable with that of free aspartic acid. The pK_{a1} of L_c is larger, possibly due to the electron donating effect of the alkyl substituent. The difference between the pK_{a1} and pK_{a2} which corresponds to the interaction between the two aspartates in a ligand, is 1.46 and 0.7 for L_b and L_c, respectively. If there were no interaction between the two aspartic moieties, the theoretical pK_a difference would be 0.3. The pK_a differences in L_b and L_c are larger than 0.3, indicating that the monoprotonated aspartic acid interacts with the other aspartate in L_b. The pK_{a3} and pK_{a4} of L_b and L_c correspond to pK_{a2} of free aspartic acid. They are 4.19 and 3.62 and 3.93 and 3.15 for L_b and L_c, respectively, which is similar to 3.71 in free aspartic acid. The second protonation constant of aspartate in L_b is slightly larger than that in L_c. The pK_{a5} and pK_{a6} for L_b is 2.75 and 2.39. When the concentration effect is taken into consideration, they are almost the same, which indicates that the fully protonated aspartates in L_b have no interaction with each other. The pK_{a5} and pK_{a6} in L_c are smaller than 2.0 (third protonation constant of free aspartic (1.9)), therefore, the log β_5 and log β_6 have a much larger error than any of the other protonation constants. The pK_{a5} and pK_{a6} of L_c are so close that protonation takes place simultaneously. The protonation process is illustrated in Scheme 2. The distribution diagrams are shown in Fig. 3.

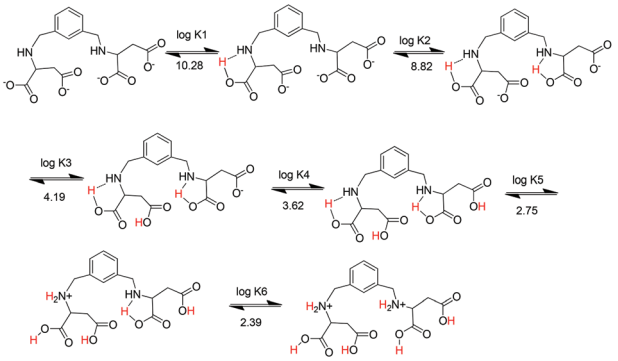

Scheme 2 Protonation process of L_b in aqueous solution at 25 °C, I = 0.10 M KNO_3.

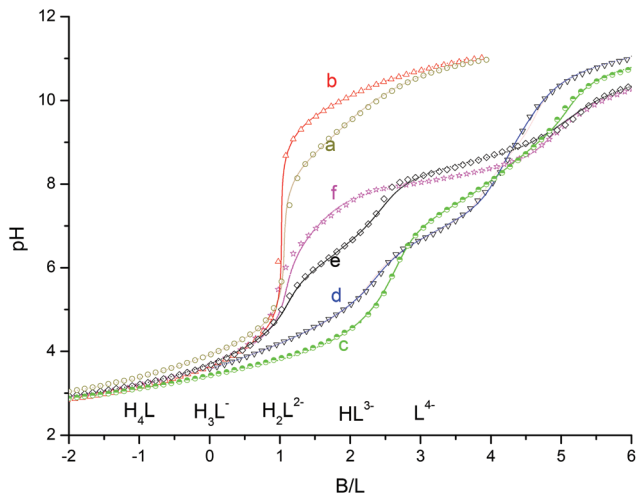

Fig. 2 pH titration curve of 1.000 × 10^{-3} M ligand in the absence and presence of 2.000 eq. metal ions at 25.0 ± 0.1 °C, I = 0.10 M KNO_3. B/L is the molar ratio of base to ligand. Lines are simulated data, symbols are experimental. (a) 1.000 × 10^{-3} M L_b; (b) 1.000 × 10^{-3} M L_c; (c) 1.000 × 10^{-3} M L_b and 2.000 × 10^{-3} M $Cu(NO_3)_2$; (d) 1.000 × 10^{-3} M L_c and 2.000 × 10^{-3} M $Cu(NO_3)_2$; (e) 1.000 × 10^{-3} L_b and 2.000 × 10^{-3} M $Zn(NO_3)_2$; (f) 1.000 × 10^{-3} L_c and 2.000 × 10^{-3} M $Zn(NO_3)_2$.

The titration curves in the presence of 2 eq. Zn^{2+} or Cu^{2+} are significantly different from those in the absence of metal ions (Fig. 2). Upon removal of all protons from the ligand at B/L = 3, the pH is roughly 6 and 8 in the presence of 2 eq. Cu(II) and 2 eq. Zn(II), respectively. With further addition of base, the pH did not increase sharply, which indicates that OH^- is coordinated to the metal ion. Both complexes have a pH jump at B/L = 5, which means two more protons from each ligand are dissociated in the presence of 2 eq. of metal ions. These two protons must come from coordinated water molecules. If the complex species $M_pL_qH_r$ are represented by pqr, species (21$\bar{2}$) exists in weak basic solutions. Scmar simulations reveal that the two ligands formed dinuclear complexes with different protonation modes. The formation constants (log K) of species $M_pL_qH_r$, are summarized in Table 2. Note that r can be a negative integer, which means r extra protons have dissociated from the species. These stability constants are comparable with those reported recently by Miličević[35] for Zn(II)–aspartic acid complexes with log K_{110} = 5.42. Claridge reported the log K_{110} of aspartate–copper(II) complex to be 8.84 in I = 0.1 M KNO_3 at 25 °C.[36] These data are comparable with recently reported data by Sajadi.[34]

The log K of L_b complex 210 is 17.25 and 11.93 for Cu^{2+} and Zn^{2+}, complexes, respectively, which are roughly similar to complexes of free aspartic acids. These data are 17.54 and 10.57 for L_c Cu^{2+} and Zn^{2+} complex. For both ligands, the titration curves of Cu(II) complexes are always below those of Zn(II) complexes (Fig. 2). The titration curves of L_b and its complexes are given later of corresponding L_c analogs in B/L < 3. At B/L = 3 or higher, the relative position of the titration curves are

Table 1 The cumulative protonation constants of ligands at I = 0.10 M KNO_3, 25 °C

Ligand	log β_1	log β_2	log β_3	log β_4	log β_5	log β_6
L_b	10.28(02)	19.10(03)	23.29(05)	26.91(05)	29.66(07)	32.05(09)
L_c	10.54(06)	20.38(05)	24.31(07)	27.46(07)	NA[a]	31.94(13)

[a] The error in β_5 is much larger than any other species.

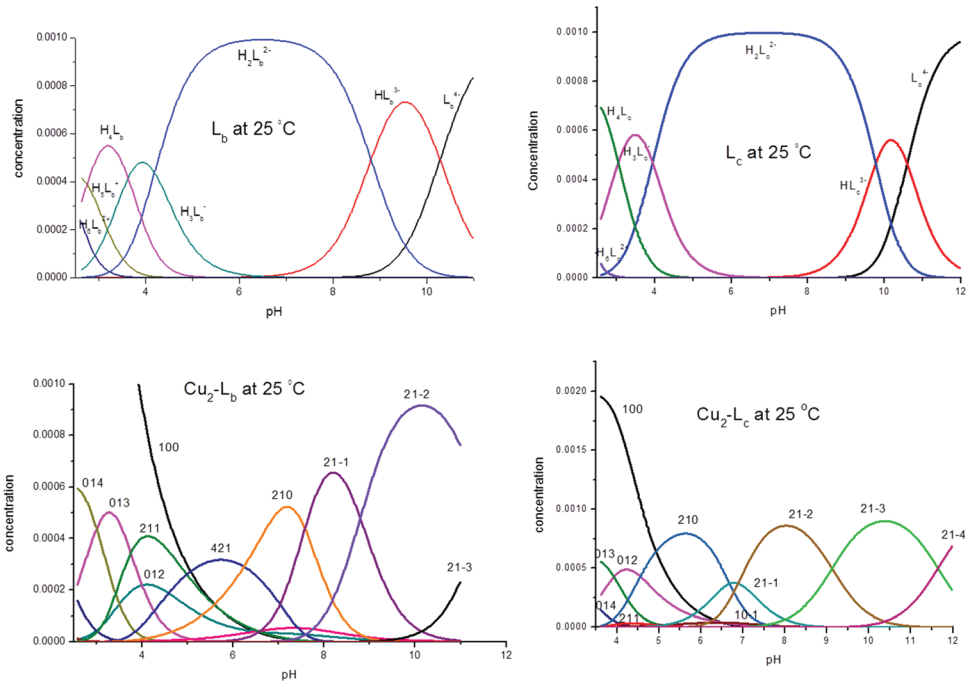

Fig. 3 Distribution curve of 1.00×10^{-3} M ligands (top) and their copper(II) complexes (2.00×10^{-3} M $Cu(NO_3)_2$) (bottom) in aqueous solution at 25 °C, I = 0.10 M KNO_3.

Table 2 Species and their stability constants (log K) of L_b and L_c complexes at 25 °C, I = 0.10 M KNO_3

Species $(pqr)^a$	2Cu–L_b	2Zn–L_b	2Cu–L_c	2Zn–L_c
211	22.84(03)	19.66(09)	21.75(09)	18.72(08)
210	17.25(09)	11.93(13)	17.54(04)	10.57(09)
21	9.67(10)	4.08(05)	10.86(07)	
21$\bar{2}$	0.88(09)	−4.92(09)	3.88(07)	−5.16(05)
21$\bar{3}$	−10.62(15)	−15.58(11)	−5.34(19)	−15.44(06)
21$\bar{4}$	NA	−26.38(14)	−16.98(34)	−25.95(08)
421	44.28(10)	36.66(09)	NA	NA

[a] Species $M_pL_qH_r$ is presented as pqr.

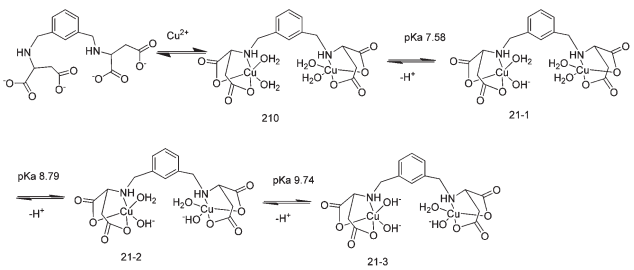

Scheme 3 The coordination process of L_b with Cu^{2+} in aqueous solution at 25 °C, I = 0.10 M KNO_3.

reversed. This phenomenon is observed because the coordinated water molecule has a lower pK_a in L_c complexes than in L_b complexes. The log K difference between adjacent species, such as log K (210) and log K (21$\bar{1}$), is the pK_a of the coordinating water molecule. The coordinated water molecules in 2Cu–L_b have pK_a of 7.58 and 8.79 (Scheme 3), while 2Cu–L_c complex have pK_a 6.68 and 6.98 respectively. For 2Zn–L_b complex, they are 7.85 and 9.00. The species distribution is shown in Fig. s7–s10.† There is some dimerized species (421) for L_b–2Cu complex in weakly acidic solution (Fig. 3).[37] We have tried different methods to isolate a solid complex, but unsuccessfully. The complexes are highly soluble in water in pH 7–9 region, but insoluble in organic solvents.

Based on the titration data, the coordination process and the pK_a of coordinated species are summarized in Scheme 3.

Acid–base has been a common term in chemistry for a long time. For Lewis acid–base adducts, their stability constants can be considered as the interaction strength between the Lewis acid and the Lewis base. Sigel *et al.* have published many papers that deal with pK_a and/or stability constants.[38] Although, the pK_a or log K value is the absolute interaction strength, there are still no relative criteria to characterize how strong the interaction is between acid and base. Here we propose a parameter that can easily characterize the relative strength of an acid or base. The most common substance related to acid–base chemistry is water. The binding constant between a standard acid, H^+, and a standard base, OH^-, is 1.0×10^{14}. Other ligands (bases) bind to protons in the same way but with a different binding constant. The binding constant is a measurement of the interaction between the acid and the base. We define the binding constant 1.0×10^{14}, as the binding strength between a standard base (ligand) and a standard acid (metal ion) (Scheme 4). Then σ = log K/14 represents the binding strength between an acid and a base (Scheme 4). Especially, when the acid is H^+, the log K/14 represents the

$H^+ + B \overset{K_b}{\rightleftharpoons}$ product $\log K_b/14$ (relative basicity of B to OH^-)

$A + OH^- \overset{K_a}{\rightleftharpoons}$ product $\log K_a/14$ (relative acidity of A to H^+)

$A + B \overset{K_f}{\rightleftharpoons}$ product $\log K_f/14$ (relative binding strength to H-OH)

Scheme 4 The definition of relative binding strengths.

basicity of a ligand. When the base is OH^-, the log K/14 represents the acidity of a cation (metal ion). According to this definition, the basicity of acetate (pK_a = 4.75) is 0.339, or the binding strength between a proton and acetate is 33.9% that of the HO–H bond. For L_b, the pK_{a1} is 10.28, equivalent to σ = 0.734, which indicates that the L_b^{4-} has 73.4% the basicity of OH^-. For L_c, the pK_{a3} is 4.19, which indicates that $H_2L_c^-$ has 29.9% the basicity of OH^-. The pK_{a1} and pK_{a2} difference (corresponding to the pK_{a1} difference in the two aspartates in a ligand) is 1.46 and 0.70 for L_b and L_c, respectively. Taking the concentration effect (log 2 = 0.30) into account, the difference is 1.06 and 0.40, or σ = 0.076 and 0.029 in L_b and L_c, respectively. This means that the interaction between the mono-protonated aspartate and un-protonated aspartate is 7.6% and 2.9% the strength of H^+ and OH^- in L_b and L_c respectively.

The linear free energy relationship (LFER) exists in coordination chemistry, which is expressed as $\log K_{ML} = a\log K_{HL} + b$, where K_{ML} is the stability constant of complex ML, K_{HL} is the protonation constant of ligand L, a and b are constants. This relationship can be re-written as: $\sigma_{ML} = a\sigma_{HL} + b/14$, which indicate the binding strength between ligand and metal ion is proportional to the binding strength of ligand and proton. Explaining LFER with relative binding strength is more understandable and meaningful.

Reaction with H_2O_2 in aqueous solution

As shown in Fig. s8,† in the presence of H_2O_2, the solution pHs are lower (the titration curve is in the bottom) than in the absence of H_2O_2. This indicates that more protons are dissociated and H_2O_2 reacted with the complex. H_2O_2 cannot react with the dinuclear complex if the pH is less than 6.3. Therefore, the reaction of H_2O_2 and copper complex was studied in weak basic solution.

m-Xylyl bridged dinuclear complexes are somewhat similar to the active center of hemerythrin and hemocyanin. It was found that dioxygen activation of the di(2-pyridylmethyl) amine substituted xylene copper(I) complex led to ligand hydroxylation.[21] Some similar results were also reported later.[21,22] Ligand hydroxylation also takes place in iron complexes of iminodiacetate substituted analogs.[23] Fig. 4 shows the UV-vis spectral changes after adding H_2O_2 to 1.50×10^{-3} M Cu_2–L_b complex at pH 7.5 aqueous solution. The complex is essentially colorless. After adding H_2O_2, it becomes yellow. A new absorption band appeared at 360 nm. This peak is possibly the ligand hydroxylated complex.[39] The intensity of the peak depends on pH. High pH will increase the 360 nm

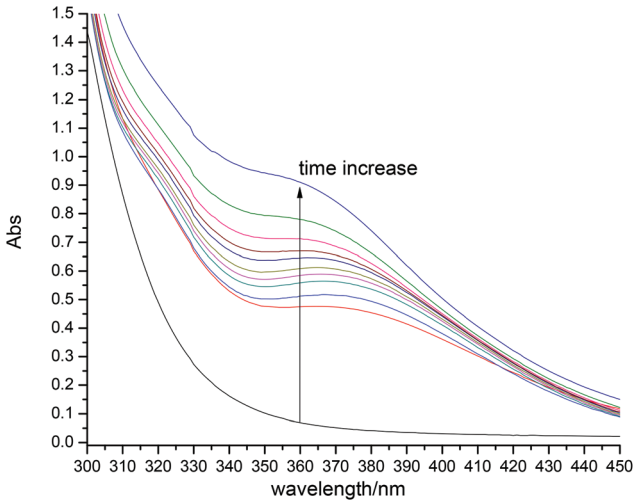

Fig. 4 Spectral changes recorded for the reaction of 1.5×10^{-3} M L_b–2Cu with 0.08 M H_2O_2 in pH = 7.50, 0.2 M KH_2PO_4–NaOH-solution at room temperature.

absorbance. The 360 nm absorbance coefficient is 660 L mol^{-1} cm^{-1} at 0.20 M pH 7.5 phosphate buffer. At pH 9.0 tetraborate buffer, the oxidized product has an absorbance coefficient ~3.2×10^4 L mol^{-1} cm^{-1}. Phosphate buffers significantly decrease the absorbance of the oxidized product. The 360 nm absorbance also decreases with the decrease of pH. This is possibly due to phosphate acting as a ligand that prevents it from binding to H_2O_2. The 360 nm absorbance decreases in the presence of buffers, whether phosphate or borax compared with the same pH without buffer. Borax buffer decreases the 360 nm absorbance less significantly than that of phosphate buffer at the same pH. Although the spectra change is much more obvious without any buffers, but H_2O_2 reaction with dinuclear copper(II) complex will decrease the pH of the solution 0.8–1 units, so all the reactions were run in buffer solution (Fig. s8†). L_c–2Cu complex has a similar reaction except the 360 nm peak is not that obvious (Fig. s9†) in pH 7.5 phosphate buffer, but the 360 nm peak is much more obvious in pH 8.5 borax buffer.

The 360 nm absorbance increase in the presence of excess H_2O_2 in phosphate buffers (Fig. s10†). The equation for a first-order reaction is $kt = \ln[(A_\infty - A_0)/(A_\infty - A_t)]$, where k_{obs} is the observed rate constant, A_∞, A_t and A_0 are the 360 nm absorbance at time ∞, t and 0. Plots of $\ln[1/(A_\infty - A_t)]$ *vs.* t give straight lines, where the slope of the line is the first-order rate-constant k_{obs}. The catalytic oxidation is first-order to L_c–2Cu complex which can be expressed as $v = k_{obs}[L_c\text{–}2Cu]$. However, for the L_b–2Cu complex, this plot is not linear. For the L_b–2Cu complex, the plot $1/(A_\infty - A_t)$ *vs.* t gives a very good straight line, which indicates the oxidation is second-order to L_b–2Cu complex, *i.e.* $v = k_{obs'}[L_b\text{–}2Cu]^2$. Tables 3 and 4 listed the observed second-/first-order rate constants for 5×10^{-4} M L_b–/L_c–2Cu in 0.02 M phosphate buffer at 25 °C, pH = 7.50.

Not only do complex concentrations have an influence on the reaction rate, but also on H_2O_2. For complex L_c–2Cu, the observed first-order rate constants k_{obs} increase linearly with

Table 3 The observed second-order rate-constant (L mol^{-1} s^{-1}) of 5×10^{-4} M L_b–2Cu in 0.02 M phosphate buffer at pH 7.5, 25 °C at different H_2O_2 concentrations

$[H_2O_2]$	0.0015	0.025	0.10	0.18	0.25	0.40
2nd-order $k_{obs'}$	0.037 ± 0.0001	0.16 ± 0.0005	0.25 ± 0.001	0.30 ± 0.003	0.32 ± 0.002	0.33 ± 0.002

Table 4 The observed first-order rate-constant (s^{-1}) of 5×10^{-4} M L_c–2Cu in 0.02 M phosphate buffer at pH 7.5, 25 °C at different H_2O_2 concentrations

$[H_2O_2]$	0.1	0.175	0.25	0.325	0.4
1st-order k_{obs}	$(8.1 \pm 0.02) \times 10^{-4}$	$(2.9 \pm 0.006) \times 10^{-3}$	$(4.4 \pm 0.02) \times 10^{-3}$	$(7.6 \pm 0.02) \times 10^{-3}$	$(8.4 \pm 0.06) \times 10^{-3}$

the increase of H_2O_2 concentrations (Table 4). The rate law for L_c–2Cu complex was:

$$v = k[H_2O_2][L_c\text{–}2Cu], k = 0.02294 \pm 0.00231 \text{ L mol}^{-1} \text{ s}^{-1}. \quad (1)$$

While for L_b–2Cu, $v = k_{obs'}[L_b\text{–}2Cu]^2$. The $k_{obs'}$ *vs.* $[H_2O_2]$ is not a straight line (Fig. s11†). However, the plot of $1/k_{obs'}$ *vs.* $1/[H_2O_2]$ is a straight line (Fig. s11†). That is $1/K_{obs'} = a + b/[H_2O_2]$, where a and b are the intercept and slope of the line.

Rearranging:

$$k_{obs'} = [H_2O_2]/(b + a[H_2O_2]) = [H_2O_2]/(0.087 + 2.89[H_2O_2])$$

The rate-law for the reaction of L_b–2Cu with H_2O_2 in 0.020 M pH 7.5 phosphate buffer can be written as:

$$v = k_{obs'}[L_b\text{–}2Cu]^2 = [L_b\text{–}2Cu]^2[H_2O_2]/(0.087 + 2.89[H_2O_2]) \quad (2)$$

The rate-law for the reaction of L_b–2Cu and L_c–2Cu with H_2O_2 is different, which indicates a different mechanism. pH has a great influence on the reaction rate. Increasing pH will increase the 360 nm absorbance of the products. Increasing pH will also make the reaction faster between dinuclear copper(II) complexes and H_2O_2. The reaction is too fast to study the kinetics by UV-vis in pH > 9. After a longer reaction time at high pH precipitation will occur. The reaction mechanism needs further exploration.

Radical trapping test

The very high reactivity of the $OH^{\cdot}$ radical enables it to react with a wide range of molecules found in living cells, such as sugars, amino acids, lipids and nucleotides. Although $OH^{\cdot}$ formation can occur in several ways, by far the most important mechanism *in vivo* is the Fenton reaction, where a transition metal is involved as a pro-oxidant in the catalyzed decomposition of superoxide and hydrogen peroxide. With this assay, the 500 nm absorbance changed due to hydroxyl radical scavenges/releases in the presence of copper(II) complexes than in the absence of the copper(II) complexes (Fig. s13†). $OH^{\cdot}$ radical scavenged 4.2% and 2.6% in the presence of L_b–2Cu and L_c–2Cu respectively (the spectra were measured immediately, Table 5). After 30 min reaction in dark, radicals scavenged are 4.7% and 12% for L_b–2Cu and L_c–2Cu respectively (Table 5). L_c–2Cu can scavenge twice as many $OH^{\cdot}$ radicals than that of L_b–2Cu in the presence of H_2O_2.

Table 5 $H^{\cdot}$ [a] and $OH^{\cdot}$ [b] radical scavenging/formation data of the dinuclear complexes

		A_0 [c]	A_1 [d]	A_2 [e]	Radical increased (%)
DPPH radical	L_b–2Cu [f]	0.755	0.736	0.003	2.9
	L_c–2Cu [f]	0.755	0.421	0.006	45.0
OH radical	L_b–2Cu [g]	1.022	1.156	0.091	−4.2
	L_c–2Cu [g]	1.022	1.124	0.075	−2.6
	L_b–2Cu [f]	0.827	1.011	0.145	−4.7
	L_c–2Cu [f]	0.827	1.043	0.119	−11.7

[a] 545 nm absorbance of 1.33×10^{-2} M H_2O_2, 1.0×10^{-4} M DPPH, 1.67×10^{-4} M L–2Cu in methanol–H_2O (1 : 2). [b] 500 nm absorbance of 5.0×10^{-4} M $FeSO_4$, 1.4×10^{-3} M H_2O_2, 2.0×10^{-3} M sodium salicylate and 8.3×10^{-5} M L–2Cu mixture. [c] A_0 was the absorbance of the control (without copper(II) complex). [d] A_1 was the absorbance in the presence of the copper(II) complex. [e] A_2 was the absorbance without sodium salicylate/DPPH. [f] Measured after 30 min in dark. [g] Measured immediately after mixing.

DPPH assay is routinely used for assessment of the free radical scavenging potential of an antioxidant molecule and considered as one of the standard and easy colorimetric methods for the evaluation of antioxidant properties.[40] The highly reactive $H^{\cdot}$ radical can react with DPPH radical by donating hydrogen to a free DPPH radical and hence its reduction to an unreactive colorless species.[41] Addition of hydrogen removes the odd electron feature which is responsible for radical reactivity (DPPH color fades, Fig. s14†). The L_b–2Cu complex fades 2.9% of DPPH absorbance at 545 nm. While L_c–2Cu complex decreases 45% of the DPPH radical absorbance. These data indicate that both complexes scavenge the $OH^{\cdot}$ radical, but generate the $H^{\cdot}$ radical. L_c–2Cu can generate the $H^{\cdot}$ radical much more effectively than that of the L_b–2Cu complex when reacted with H_2O_2. This may explain why the reaction kinetics of the two dinuclear complexes is different.

We expect there should be some $OH^{\cdot}$ radical generated upon reaction with H_2O_2.[19g,42] However, the sodium salicylate–Fe(II) system gives a negative result. EPR spectra indicate that reactive oxygen species (ROS) can generate $H^{\cdot}$ radical.[43] Recently, Yuzawa[44] proposed a $H^{\cdot}$ radical generation mechanism in acidic and basic aqueous solution. ROS (S···H–$O^{\cdot}$, where S is organic substrate) gives an electron to H^{+} to

generate the $H^{\cdot}$ radical. From literature data, $H^{\cdot}$ does exist in the presence of ROS.

Mass spectra

The UV-vis spectra indicate that dinuclear copper(II) complexes of L_b and L_c react with H_2O_2 in neutral or basic aqueous solution. Radical scavenging/formation tests, as discussed above, showed that the reaction mechanism is different for the two complexes. The likely product was possibly a xylyl hydroxylated species. The reaction was monitored by MS spectroscopy.

The negative ion ESI-MS of L_b–2Cu complex in aqueous solution at pH 7 and 9 before and after adding H_2O_2 are shown in Fig. 5. The main peaks are essentially the same at pH 7 and 9 except the 606 and 608 peak in pH 7 did not appear in pH 9. The strongest peak at 561 and 563 is $[Cu_2L_b(OH)(H_2O)_3]^-$ (M^-), and has an isotope pattern identical to simulation. This formula agrees well with the pH titration data. Besides these peaks, the L_b–2Cu complex also shows $M^- - 3H_2O$ peaks at 505 and 507; $M^- + KNO_3$ at 662 and 664; $M^- + 2KNO_3$ at 763 and 765. The 606 and 608 peak is $[Cu_2L_b(NO_3)(H_2O)_3]^-$. The 707 and 709 peak in pH 7 is $[Cu_2L_b(NO_3)(H_2O)_3]^- + KNO_3$. After adding H_2O_2, the dinuclear complex revealed the presence of corresponding $Cu_2L + O$ (+16) peaks. This is possibly due to the replacement of OH^- by HOO^-, or the hydroxylation of the phenyl in the 2-position to form the phenol group. Ligand hydroxylation in the presence of H_2O_2 is well established in xylyl-containing dinuclear iron(III) and Cu(II) complexes.[23,45] The same conclusions were drawn from the positive ion spectra (Fig. s18†), and this also agrees well with the distribution curve of the system.

The MS spectra of L_c–2Cu complex is quite complicated (Fig. s16†). In contrast to the L_b–2Cu complex, no mono-oxygenated peaks (+16) were present, but instead dehydrogenation of the cyclohexane occurred in the presence of H_2O_2. Ligand hydroxylation is common in xylyl-containing ligands, but is impossible in cyclohexane-containing ligands within several minutes. Ligand dehydrogenation takes place in air without adding H_2O_2. This might explain why the L_c–2Cu complex decreased the DPPH absorbance much more effectively than the L_b–2Cu complex.

Analysis of fully oxidized products

The mass spectra (Fig. 5 and s16†) discussed in the previous section are those of the complexes obtained immediately after adding H_2O_2. To investigate the final products of H_2O_2 oxidation, 20 μL of 30% H_2O_2 was added to 2.0 mL of dinuclear copper(II) complex of L_b and L_c (pH 9.0). After stirring the mixture for 1 h, 50 μL of 0.08 M K_2S solution was added. The mixture was left at room temperature for 1/2 h. CuS was removed by centrifugation before HPLC-MS measurements were obtained. Although there are more than 2 oxidized species for L_b complex, HPLC was not able to separate them well and only one peak appeared in the HPLC. However, the oxidized form of L_c was separated in two parts in a 2 : 1 ratio. The major part of the oxidized form of L_c was identical to the oxidized form of L_b (Fig. 6).

Aspartic acid oxidation is a common phenomenon that takes place in biological systems. The product of aspartic acid oxidation is the keto acid,[46] and the intermediate is an imino compound. Amino hydroxylation was also reported recently.[47]

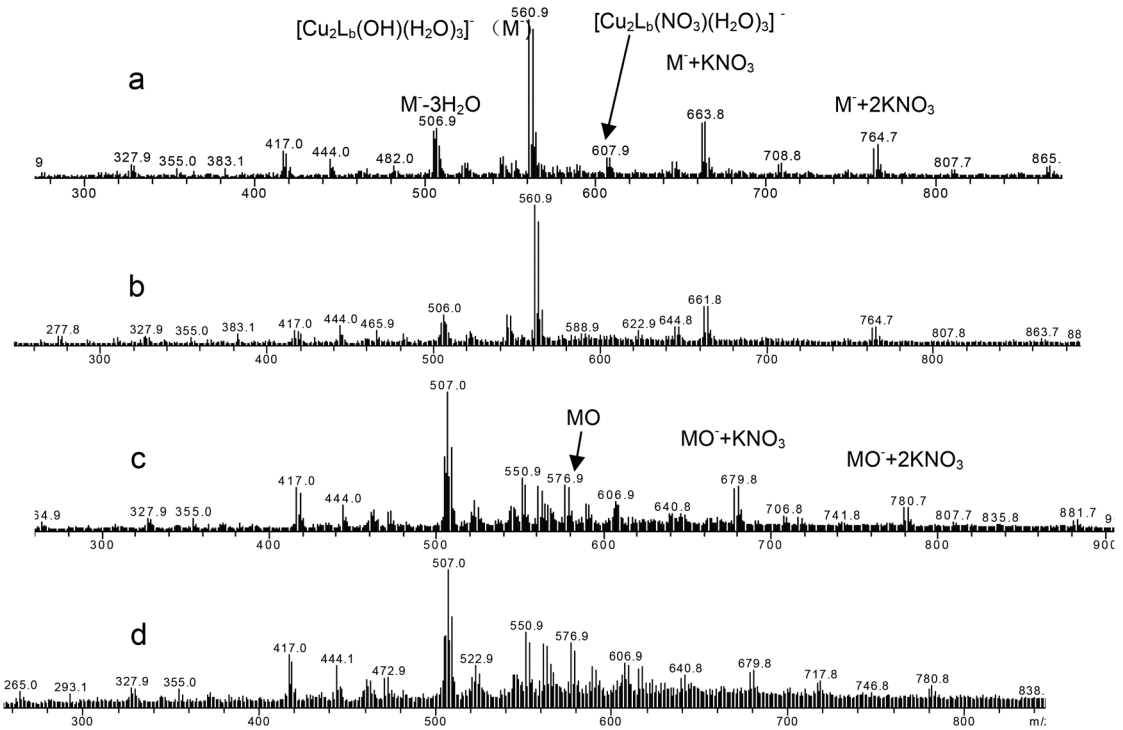

Fig. 5 L_b–2Cu negative ion mass spectrum (a) pH 7, (b) pH 9, (c) pH 7 – H_2O_2 (d) pH 9 – H_2O_2.

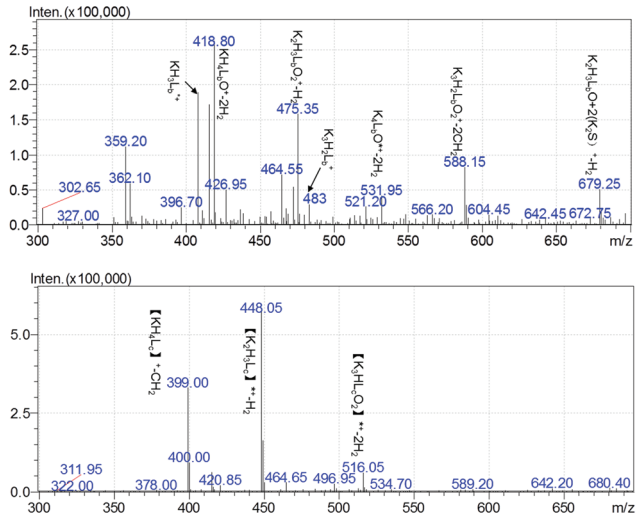

Fig. 6 The MS of L_b– and L_c–2Cu after oxidation overnight in the presence of excess H_2O_2. Cu(II) was removed by K_2S. (top) L_b; (bottom) L_c minor part.

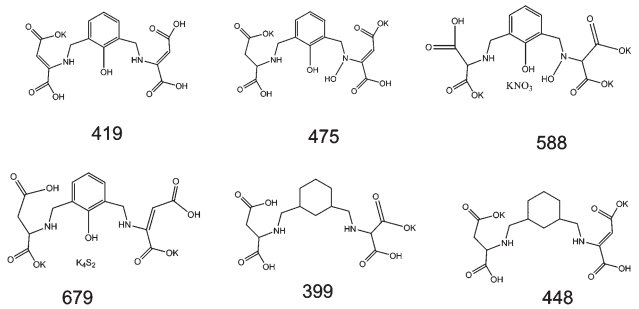

Scheme 5 Proposed ligand oxidation products and their m^+/z values.

For L_b–2Cu complex, the un-oxidized ligand had $K_3H_2L_b^+$ peaks at 483, $K_3H_2L_b^+$–H_2O at 465, $K_2H_3L_b^+$–H_2O at 427 and $KH_4L_b^+$ at 407. The strongest peak at 419 is the mono-oxygenated form of the ligand, $[KH_4L_bO]^+$–$2H_2$, whose structure is illustrated in Scheme 5. The 416 peak is $KH_3L_bO^*$–$3H_2$ radical. Peaks at 475 and 588 are the doubly oxygenated species, $K_2H_3L_bO_2^+$–H_2 and $K_3H_2L_bO_2^+$–$2CH_2$, respectively (Scheme 5). Dehydrogenation of an alkyl group will generate a double bond, the position of the double bond is not clear yet. The proposed structures are similar to those reported by Zhu *et al.*[19g] The amount of minor HPLC band of the oxidized form of L_c is roughly 1/2 that of the major band. Because the MS of the major band was identical to the MS of L_b, it was concluded that the cyclohexane moiety of L_c had been oxidized to a phenyl ring. The MS spectrum of the minor part indicated the presence of a different structure. The base peak at 448 is $K_2H_2L_c^{*+}$–H_2. The decarboxylated form (–CH_2) is located at 399, which corresponds to $KH_4L_c^+$–CH_2. The 516 peak is attributed to the double oxygenated form, $K_3HL_cO_2^+$–$2H_2$. Isotope patterns are identical to the theoretical simulations. According to the above discussion, L_b hydroxylation at the 2-position of the xylyl is the predominant species. Ligand L_b can be doubly oxygenated and dehydrogenated as well. While for L_c, full dehydrogenation of the cyclohexyl group will generate L_b in its oxidized form. Incomplete oxidation of L_c will generate decarboxylated and oxygenated products. We tried our best to separate these mixtures by chromatography, but failed. Possible oxidation products are illustrated in Scheme 5.

Catalytic oxidation of nitrobenzene

Considering its high oxidation potential, it would appear unlikely that activation of nitrobenzene would proceed by oxidation *via* electron transfer. In fact, nitrobenzene has been observed to be a mild oxidative dehydrogenating agent under both acidic and basic conditions.[48] The oxidation of nitrobenzene is quite difficult. A Scifinder search gives 17 references on nitrobenzene oxidation into nitrophenol. The most closely related studies to our work are the vanadium(v)-substituted polyoxometalates[49] and iron-catalyzed[50] oxidation of nitrobenzene into nitrophenol. Both reactions are heterogeneous with long reaction times and low conversions (<10%), and a free radical mechanism is proposed. Anodic oxidation can also oxidize nitrobenzene into nitrophenol with 18% yield.[51] Cumyl hydroperoxide[52] can oxidize nitrobenzene in strong basic media with yield 45%. The reaction proceeds *via* an addition-base-induced β-elimination pathway analogous to that of vicarious nucleophilic substitution. Most of the oxidations are non-selective even protein engineering.[53] D'Oliveira found that UV-illuminated TiO_2 in the presence of O_2 (air) can oxidize nitrobenzene into nitrophenol.[54] To our knowledge, investigations of the reaction kinetics are still rare and ambiguous.

Upon addition of H_2O_2, nitrobenzene is oxidized quickly to nitrophenol as indicated by its absorbance at 400 nm. In 0.20 M phosphate buffer, no observable pH change was observed before and after catalytic oxidation. Fig. 7 illustrates the spectral changes that occurred during catalytic oxidation of 0.80×10^{-3} M nitrobenzene by 0.1667 M H_2O_2 in 0.2 M KH_2PO_4 buffer at pH = 8.00, by 2.08×10^{-5} M L_c–2Cu complex.

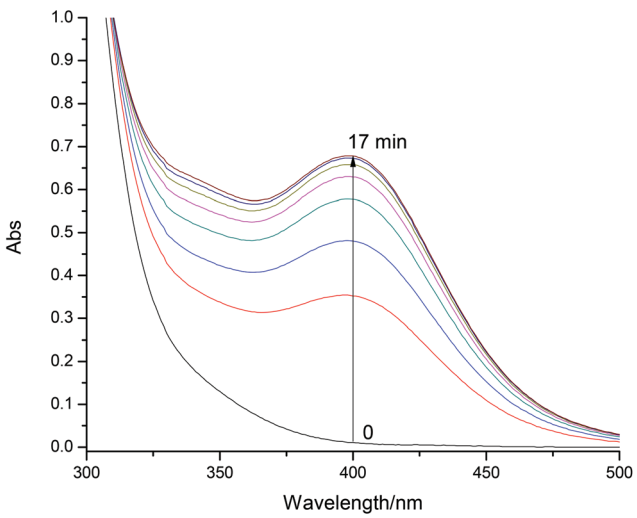

Fig. 7 Spectral changes with time recorded for the reaction of 0.8×10^{-3} M nitrobenzene and 2.08×10^{-5} M L_c–2Cu with 0.1667 M H_2O_2 in pH = 8.00, 0.2 M KH_2PO_4–NaOH-solution at 25 °C.

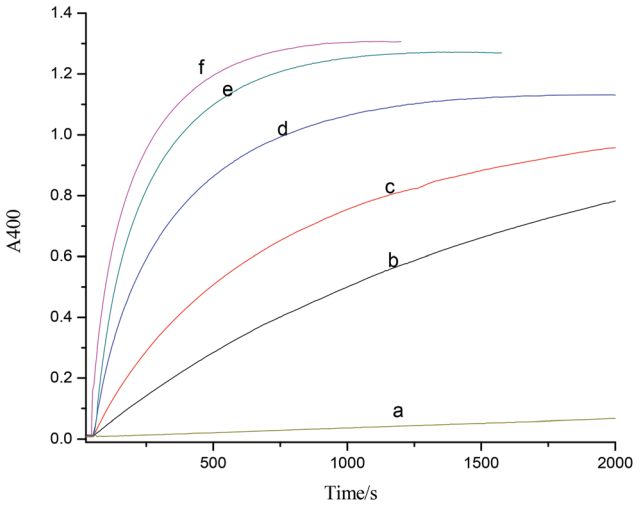

Fig. 8 Kinetic traces recorded at 400 nm for the catalyzed oxidation of nitrobenzene. Reaction conditions: pH = 8.00, 0.2 M KH_2PO_4–NaOH, 1.47×10^{-3} M nitrobenzene, 0.1667 M H_2O_2, 25 °C. (a) No complex. (b) 5.00×10^{-6} M L_c–2Cu, (c) 1.25×10^{-5} M L_c–2Cu, (d) 2.50×10^{-5} M L_c–2Cu, (e) 3.75×10^{-5} M L_c–2Cu, (f) 5.00×10^{-5} M L_c–2Cu.

The absorbance at 400 nm increased during the oxidation process. The oxidation is first order in nitrobenzene.

Kinetic traces recorded at 400 nm for the catalyzed oxidation of nitrobenzene at different complex concentrations are shown in Fig. 8. The first-order rate constant linearly increases with an increase in dicopper(II) complex concentration (Fig. 8 and Tables s1 and s2†), as well as with H_2O_2 concentration (Fig. s18, Tables s3 and s4†). Although L_b–2Cu and L_c–2Cu follow a different rate law for their reaction with H_2O_2, for the catalytic oxidation process, both complexes follow the rate law (data listed in Table 6):

$$v = k[\text{complex}][\text{nitrobenzene}][H_2O_2]$$

This agrees well with the polyoxometalate catalyzed oxidation of nitrobenzene.[49b] The k values are 211.2 ± 0.3 and 607.9 ± 1.7 $L^2\ mol^{-2}\ s^{-1}$ at pH 8.0 for L_b–2Cu and L_c–2Cu, respectively. For the same reaction under the same conditions, k was 45.01 ± 0.06 $L^2\ mol^{-2}\ s^{-1}$ when the Cu complex of 1,3-*N*,*N*,*N*′,*N*′-xylylenediamine tetraacetate was the catalyst. This agrees well with the radical generation ability of the dicopper(II) complexes. As shown in Fig. 8, even at the very low complex concentration of 5.00×10^{-6} M, which is 1/294 of the nitrobenzene concentration, the maximum absorbance at 400 nm is the same as in the presence of 5.00×10^{-5} M complex concentration. These data indicate that the complex is a catalyst, not a reactant.

The pathway for the completion of the reaction, nitrobenzene to nitrophenol is still unclear.[49b] According to radical trapping data, we believe that the oxidation of nitrobenzene occurs *via* an H˙ radical mechanism, different from the OH˙ radical mechanism proposed by Jin Anotai *et al.* in acidic aqueous solution.[16] This can also be further proved by different rate formulae for nitrobenzene oxidation *via* the Fenton process ($v = 0.259[Fe^{2+}]^{1.02}[H_2O_2]^{0.34}[NB]^{-0.094}$, where NB represents nitrobenzene, which is different from ours).[16] Our dinuclear copper(II) complexes have obvious advances over the Fenton process. Firstly, the catalytic reaction takes place in weak basic aqueous rather than the Fenton process at pH 2.4–3.6.[16] Secondly, the k for our complexes (200–600) is much larger than that of the Fenton process (0.259). Although the nitrobenzene concentration was not very high, our complexes can convert all of the nitrobenzene substrate into nitrophenol. The full conversion of nitrobenzene can be proved by the 400 nm absorbance plateau (A_∞). The plateau is irrelevant to complex (catalyst) concentrations in the experiments (Fig. 8). All other known catalytic systems have a much lower nitrobenzene conversion.[49–52]

The oxidation rate increased with an increase in the reaction temperature (Fig. s19,† Table 7). The Arrhenius activation energies, obtained from a plot of ln k *vs.* $1/T$, are 69.4 ± 2.2 and 70.0 ± 4.3 kJ mol^{-1} for L_b and L_c dicopper complexes, respectively (Fig. s20†). These values are essentially the same and also the same as 378 to 600 °C supercritical water oxidation in the absence of oxygen 68.0 ± 9.0 kJ mol^{-1}.[55] However, the Arrhenius pre-exponential factors are 2.62×10^{14} and 1.06×10^{15} respectively. These pre-exponential factors are significantly larger than that for supercritical water oxidation.[55] It is the larger pre-exponential factor that make the L_c–2Cu complex more active than the L_b–2Cu complex in nitrobenzene catalytic oxidation.[56]

The rate of nitrobenzene oxidation is also affected by pH of reaction solution (Table 8). An increase in the reaction pH significantly increased the oxidation rate. This phenomenon agrees well with the reaction between the complexes and H_2O_2, indicating that dioxygen activation is the first step in the catalytic oxidation.

4. Conclusions

Two new bis-aspartic acid ligands were synthesized *via* Michael addition in aqueous solution. Both ligands react with Cu(II) and Zn(II) to form dinuclear complexes. pH titration, as well as ESI-MS indicates that $M_2L(OH)^-$ is the major species in neutral/weak basic aqueous solution. The dinuclear copper complexes react with H_2O_2 in aqueous solution. The reaction mechanism of the two Cu complexes differs greatly in 0.020 M pH 7.5 phosphate buffer. The oxidation products were oxygenated and/or dehydrogenated species in neutral and basic aqueous solution. Both complexes can trap/scavenge OH˙ radical, but generate H˙ radical when reacting with H_2O_2, especially the L_c–2Cu complex. Both complexes can catalyze nitrobenzene oxidation in the presence of H_2O_2 in weak basic aqueous solution. The two complexes follow the same rate-law. The catalytic rate constant of L_c–2Cu is 3 times that of the L_b–2Cu complex. It is the larger pre-exponential factor that make L_c–2Cu complex more active than L_b–2Cu complex in nitrobenzene catalytic oxidation. Both complexes can convert all

Table 6 The first order $k_{obs} \times 10^4$ (s^{-1}) for oxidation of 1.47×10^{-3} M nitrobenzene in the presence of 0.1667 M H_2O_2 in 0.2 M KH_2PO_4 buffer at pH = 8.00, 25 °C

[Complex]	5.00×10^{-6}	1.25×10^{-5}	2.50×10^{-5}	3.75×10^{-5}	5.00×10^{-5}	No complex
L_b–2Cu	2.25 ± 0.004	4.56 ± 0.006	8.73 ± 0.009	13.2 ± 0.02	16.9 ± 0.04	0.622 ± 0.0001
L_c–2Cu	4.21 ± 0.003	11.3 ± 0.02	26.9 ± 0.06	38.0 ± 0.1	50.0 ± 0.2	0.622 ± 0.0001

Table 7 Rate-constants k ($L^2\ mol^{-2}\ s^{-1}$) for the oxidation of nitrobenzene by H_2O_2 catalyzed by dicopper(II) complexes in 0.20 M phosphate buffer at pH = 8.00

Temp	5 °C	15 °C	25 °C	35 °C	45 °C
L_a–2Cu[a]	11.71 ± 0.01	18.37 ± 0.02	45.01 ± 0.06	159.0 ± 0.3	347.1 ± 1
L_b–2Cu	23.36 ± 0.02	76.76 ± 0.09	211.2 ± 0.3	442.3 ± 1.3	1078 ± 5
L_c–2Cu	94.51 ± 0.2	174.4 ± 0.3	607.9 ± 1.7	1496 ± 4.1	3780 ± 40

[a] L_a is 1,3-*N*,*N*,*N*′,*N*′-xylylenediamine tetraacetate.

Table 8 The k ($L^2\ mol^{-2}\ s^{-1}$) for oxidation of nitrobenzene in the presence of H_2O_2 in 0.2 M KH_2PO_4 buffer at pH = 8.00, 25 °C

pH	7.00	7.50	8.00	8.50
L_a [a]	28.64 ± 0.03	37.99 ± 0.02	45.01 ± 0.06	102.0 ± 0.2
L_b	58.69 ± 0.02	110.0 ± 0.1	211.2 ± 0.3	406.3 ± 0.9
L_c	53.17 ± 0.08	163.2 ± 0.4	607.9 ± 1.7	1152 ± 3.6

[a] L_a is 1,3-*N*,*N*,*N*′,*N*′-xylylenediamine tetraacetate.

the nitrobenzene into nitrophenol, which is possibly one of the most effective oxidation catalysts.

Acknowledgements

The project was supported by the National Natural Science Foundation of China (grant No. 20971084 and 21001073). We are also in debt to Prof. Judith Walmsley for her careful proof reading and revision. We thank Instrumental Analysis and Research Center of Shanghai University for measurements.

References

1 (*a*) C. I. C. Esteves, M. M. M. Raposo and S. P. G. Costa, *Amino Acids*, 2010, **40**, 1065–1075; (*b*) W. Li, A. Schlecker and D. Ma, *Chem. Commun.*, 2010, **46**, 5403–5420; (*c*) R. Lukajtis, A. Legowska, M. Wysocka, D. Debowski, A. Lesner and K. Rolka, *J. Pept. Sci.*, 2011, **17**, 281–287; (*d*) L. S. Monteiro, J. J. Andrade and A. C. Suarez, *Eur. J. Org. Chem.*, 2011, 6764–6772; (*e*) K. Nokihara, A. Hirata, Y. Kodama, T. Sogon, H. Aoyama, T. Ohyama, J. Pang and W.-J. Hung, *Pept. Sci.*, 2010, **47**, 282; (*f*) G. Revilla-Lopez, A. D. Laurent, E. A. Perpete, D. Jacquemin, J. Torras, X. Assfeld and C. Aleman, *J. Phys. Chem. B*, 2011, **115**, 1232–1242; (*g*) C.-M. Zeng, S. A. Kerrigan, J. A. Katzenellenbogen, C. Slocum, K. Gallacher, M. Shomali, C. R. Lyttle, G. Hattersley and C. P. Miller, *Tetrahedron Lett.*, 2010, **51**, 5361–5363.

2 X. Z. Liang, N. N. Quan, J. Wang and J. G. Yang, *Sci. China, Ser. B: Chem.*, 2009, **52**, 874–878.

3 (*a*) X. Li, X.-S. Xue, C. Liu, B. Wang, B.-X. Tan, J.-L. Jin, Y.-Y. Zhang, N. Dong and J.-P. Cheng, *Org. Biomol. Chem.*, 2012, **10**, 413–420; (*b*) Z.-W. Ma, Y.-X. Liu, P.-L. Li, H. Ren, Y. Zhu and J.-C. Tao, *Tetrahedron: Asymmetry*, 2011, **22**, 1740–1748; (*c*) T. Miura, A. Masuda, M. Ina, K. Nakashima, S. Nishida, N. Tada and A. Itoh, *Tetrahedron: Asymmetry*, 2011, **22**, 1605–1609.

4 (*a*) D. M. Roundhill, *Chem. Rev.*, 1992, **92**, 1–27; (*b*) T. E. Mueller and M. Beller, *Chem. Rev.*, 1998, **98**, 675–703; (*c*) M. Johannsen and K. A. Jorgensen, *Chem. Rev.*, 1998, **98**, 1689–1708.

5 P. S. Piispanen and P. M. Pihko, *Tetrahedron Lett.*, 2005, **46**, 2751–2755.

6 (*a*) G. Fibriansah, V. P. Veetil, G. J. Poelarends and A.-M. W. H. Thunnissen, *Biochemistry*, 2011, **50**, 6053–6062; (*b*) R. E. Viola, *Adv. Enzymol. Relat. Areas Mol. Biol.*, 2000, **74**, 295–341.

7 B. Weiner, G. J. Poelarends, D. B. Janssen and B. L. Feringa, *Chem.–Eur. J.*, 2008, **14**, 10094–10100.

8 M. S. Gulzar, M. Akhtar and D. Gani, *J. Chem. Soc., Chem. Commun.*, 1994, 1601–1602.

9 (*a*) P. Brookes and J. Walker, *J. Chem. Soc.*, 1957, 4409–4416; (*b*) M. Boros, J. Koekoesi, J. Vamos, I. Koevesdi and B. Noszal, *Amino Acids*, 2007, **33**, 709–717.

10 (*a*) Z. Li, J. B. van Beilen, W. A. Duetz, A. Schmid, A. de Raadt, H. Griengl and B. Witholt, *Curr. Opin. Chem. Biol.*, 2002, **6**, 136–144; (*b*) E. E. Chufan, S. C. Puiu and K. D. Karlin, *Acc. Chem. Res.*, 2007, **40**, 563–572; (*c*) I. V. Korendovych, S. V. Kryatov and E. V. Rybak-Akimova, *Acc. Chem. Res.*, 2007, **40**, 510–521; (*d*) L. J. Murray and S. J. Lippard, *Acc. Chem. Res.*, 2007, **40**, 466–474; (*e*) L. Que Jr., *JBIC, J. Biol. Inorg. Chem.*, 2004, **9**, 684–690; (*f*) M. Suzuki, *Acc. Chem. Res.*, 2007, **40**, 609–617; (*g*) C. E. Tinberg and S. J. Lippard, *Acc. Chem. Res.*, 2011, **44**, 280–288.

11 (*a*) A. N. Kharat, A. Bakhoda and T. Hajiashrafi, *J. Mol. Catal. A: Chem.*, 2010, **333**, 94–99; (*b*) Z. Zhang, X. Li, C. Wang, C. Zhang, P. Liu, T. Fang, Y. Xiong and W. Xu,

Dalton Trans., 2012, **41**, 1252–1258; (*c*) J. Nakazawa, H. Ogiwara, Y. Kashiwazaki, A. Ishii, N. Imamura, Y. Samejima and S. Hikichi, *Inorg. Chem.*, 2011, **50**, 9933–9935.

12 (*a*) S. Friedle, E. Reisner and S. J. Lippard, *Chem. Soc. Rev.*, 2010, **39**, 2768–2779; (*b*) P. Hlavica, *J. Inorg. Biochem.*, 2011, **105**, 1354–1364; (*c*) K. D. Koehntop, J. P. Emerson and L. Que Jr., *JBIC, J. Biol. Inorg. Chem.*, 2005, **10**, 87–93; (*d*) S. V. Kryatov, E. V. Rybak-Akimova and S. Schindler, *Chem. Rev.*, 2005, **105**, 2175–2226; (*e*) T. Matsui, M. Iwasaki, R. Sugiyama, M. Unno and M. Ikeda-Saito, *Inorg. Chem.*, 2010, **49**, 3602–3609; (*f*) M. Morikawa, *Appl. Microbiol. Biotechnol.*, 2010, **87**, 1595–1603; (*g*) R. L. Shook and A. S. Borovik, *Inorg. Chem.*, 2010, **49**, 3646–3660; (*h*) M. Suzuki, *Acc. Chem. Res.*, 2007, **40**, 609–617; (*i*) C. E. Tinberg and S. J. Lippard, *Acc. Chem. Res.*, 2011, **44**, 280–288; (*j*) W. B. Tolman and E. I. Solomon, *Inorg. Chem.*, 2010, **49**, 3555–3556.

13 (*a*) S. R. Collinson and W. Thielemans, *Coord. Chem. Rev.*, 2010, **254**, 1854–1870; (*b*) N. Mizuno and K. Kamata, *Coord. Chem. Rev.*, 2011, **255**, 2358–2370; (*c*) R. Neumann, *Inorg. Chem.*, 2010, **49**, 3594–3601; (*d*) E. O. Odebunmi and A. S. Ogunlaja, *Curr. Res. Chem.*, 2011, **3**, 16–28.

14 Y. Chang, X.-L. Shi, X.-Q. Lu and Y.-G. Wang, *Xibei Shifan Daxue Xuebao, Ziran Kexueban*, 2008, **44**, 81–85, 110.

15 L. Santagostini, M. Gullotti, R. Pagliarin, E. Monzani and L. Casella, *Chem. Commun.*, 2003, 2186–2187.

16 (*a*) J. Anotai, P. Sakulkittimasak, N. Boonrattanakij and M.-C. Lu, *J. Hazard. Mater.*, 2009, **165**, 874–880; (*b*) C. Ratanatamskul, S. Chintitanun, N. Masomboon and M.-C. Lu, *J. Mol. Catal.A: Chem.*, 2010, **331**, 101–105; (*c*) Z. K. Dzhumanova and G. N. Dalimova, *Chem. Nat. Compd.*, 2011, **47**, 419–421; (*d*) M. Kurashvili, M. Pruidze, E. Kiskeidze, T. Varazashvili, T. Ananiashvili, G. Khatisashvili and M. Gordeziani, *J. Biol. Phys. Chem.*, 2003, **3**, 45–49; (*e*) C. Ratanatamskul, S. Chintitanun, N. Masomboon and M.-C. Lu, *Fresenius Environ. Bull.*, 2010, **19**, 2665–2671.

17 (*a*) L. Guidoni, K. Spiegel, M. Zumstein and U. Roethlisberger, *Angew. Chem., Int. Ed.*, 2004, **43**, 3286–3289; (*b*) A. Chanda, A. D. Ryabov, S. Mondal, L. Alexandrova, A. Ghosh, Y. Hangun-Balkir, C. P. Horwitz and T. J. Collins, *Chem.–Eur. J.*, 2006, **12**, 9336–9345; (*c*) W. C. Ellis, C. T. Tran, R. Roy, M. Rusten, A. Fischer, A. D. Ryabov, B. Blumberg and T. J. Collins, *J. Am. Chem. Soc.*, 2010, **132**, 9774–9781.

18 (*a*) E. Ember, S. Rothbart, R. Puchta and E. R. van, *New J. Chem.*, 2009, **33**, 34–49; (*b*) E. Ember, H. A. Gazzaz, S. Rothbart, R. Puchta and E. R. van, *Appl. Catal., B*, 2010, **95**, 179–191; (*c*) S. Rothbart, E. Ember and E. R. van, *Dalton Trans.*, 2010, **39**, 3264–3272.

19 (*a*) P. L. Holland and W. B. Tolman, *Coord. Chem. Rev.*, 1999, **190–192**, 855–869; (*b*) S. Mahapatra, J. A. Halfen, E. C. Wilkinson, G. Pan, X. Wang, V. G. Young Jr., C. J. Cramer, L. Que Jr. and W. B. Tolman, *J. Am. Chem. Soc.*, 1996, **118**, 11555–11574; (*c*) A. Decker and I. Solomon Edward, *Curr. Opin. Chem. Biol.*, 2005, **9**, 152–163; (*d*) J. A. Halfen, V. G. Young Jr. and W. B. Tolman, *J. Am. Chem. Soc.*, 1996, **118**, 10920–10921; (*e*) H. Ma, M. Allmendinger, U. Thewalt, A. Lentz, M. Klinga and B. Rieger, *Eur. J. Inorg. Chem.*, 2002, 2857–2867; (*f*) W. B. Tolman, *Acc. Chem. Res.*, 1997, **30**, 227–237; (*g*) Q. Zhu, Y. Lian, S. Thyagarajan, S. E. Rokita, K. D. Karlin and N. V. Blough, *J. Am. Chem. Soc.*, 2008, **130**, 6304–6305.

20 (*a*) M. Costas, M. P. Mehn, M. P. Jensen and L. Que Jr., *Chem. Rev.*, 2004, **104**, 939–986; (*b*) Y.-M. Lee, S. Hong, Y. Morimoto, W. Shin, S. Fukuzumi and W. Nam, *J. Am. Chem. Soc.*, 2010, **132**, 10668–10670.

21 (*a*) K. D. Karlin, R. W. Cruse, Y. Gultneh, J. C. Hayes and J. Zubieta, *J. Am. Chem. Soc.*, 1984, **106**, 3372–3374; (*b*) K. D. Karlin, J. C. Hayes, Y. Gultneh, R. W. Cruse, J. W. McKown, J. P. Hutchinson and J. Zubieta, *J. Am. Chem. Soc.*, 1984, **106**, 2121–2128.

22 (*a*) E. Pidcock, H. V. Obias, C. X. Zhang, K. D. Karlin and E. I. Solomon, *J. Am. Chem. Soc.*, 1998, **120**, 7841–7847; (*b*) K. D. Karlin, M. S. Nasir, B. I. Cohen, R. W. Cruse, S. Kaderli and A. D. Zuberbuehler, *J. Am. Chem. Soc.*, 1994, **116**, 1324–1336.

23 H. Furutachi, M. Murayama, A. Shiohara, S. Yamazaki, S. Fujinami, A. Uehara, M. Suzuki, S. Ogo, Y. Watanabe and Y. Maeda, *Chem. Commun.*, 2003, 1900–1901.

24 (*a*) D. Huang, B. Ou and R. L. Prior, *J. Agric. Food Chem.*, 2005, **53**, 1841–1856; (*b*) C. Sanchez-Moreno, *Food Sci. Technol. Int.*, 2002, **8**, 121–137; (*c*) H. Wang, X. D. Gao, G. C. Zhou, L. Cai and W. B. Yao, *Food Chem.*, 2008, **106**, 888–895.

25 (*a*) S. Zhu, F. Kou, H. Lin, M. Lin and Y. Chen, *Inorg. Chem.*, 1996, **35**, 5851–5859; (*b*) S. Zhu, A. Matilla, J. M. Tercero, V. Vijayaragavan and J. A. Walmsley, *Inorg. Chim. Acta*, 2004, **357**, 411–420.

26 H. Sun, Ph.D. Thesis, Nankai University, 1998.

27 R. de Levie, *J. Chem. Educ.*, 2010, **87**, 1188–1194.

28 (*a*) J. Fuentes, R. Reboso and A. Rodriguez, *Polyhedron*, 1989, **8**, 2693–2699; (*b*) J. Fuentes, R. Reboso and A. Rodriguez, *Polyhedron*, 1989, **8**, 1365–1370; (*c*) A. Rodriguez, R. Reboso and J. Fuentes, *An. Quim.*, 1993, **89**, 691–695.

29 (*a*) R. Endo and M. Takayanagi, JP10251208A, 1998; (*b*) T. Endo, R. Takahashi and Y. Hashimoto, EP731171A2, 1996; (*c*) M. Kaneko, Y. Hashimoto, T. Endo, M. Kato and W. Mizunashi, EP805211A2, 1997; (*d*) H. Seki, JP06130587A, 1994; (*e*) H. Seki, JP06130612A, 1994; (*f*) D. A. Wilson and D. K. Crump, WO9428464A1, 1994.

30 (*a*) R. Crovetto, C. C. Pierce and P. D. Deck, *WO Pat.*, 2010062461, 2010; (*b*) T. Inaba, S. Hirano and K. Morimoto, *EP Pat.*, 851287, 1998.

31 C. Kezerian and W. M. Ramsey, US3158635, 1964.

32 (*a*) L. Ge and L. Sun, CN101074280A, 2007; (*b*) F. Sun, CN101024618A, 2007; (*c*) X.-Z. Liang, S. Gao and J.-G. Yang, *Chem. Res. Chin. Univ.*, 2009, **25**, 744–747; (*d*) Y. Okada,

T. Banno, K. Toshima and S. Matsumura, *J. Oleo Sci.*, 2009, **58**, 519–528; (*e*) S.-C. Xue, F.-C. Xi, J.-Z. Feng, X.-Q. Chen, Q.-C. Li and G.-W. Wang, *Xiandai Tuliao Yu Tuzhuang*, 2009, **12**, 1–4; (*f*) N. N. Quan, S. H. Bao and J. G. Yang, *Chin. Sci. Bull.*, 2010, **55**, 2512–2516; (*g*) B. Zhang and X. Wang, CN101659624A, 2010.

33 D. R. Lide, *Handbook of chemistry and physics*, 88th edn, 2007, pp. 8–33.

34 (*a*) S. A. A. Sajadi, *Nat. Sci.*, 2010, **2**, 85–90; (*b*) S. A. A. Sajadi, *Adv. Biosci. Biotechnol.*, 2010, **1**, 362–368.

35 A. Milicevic and N. Raos, *J. Mol. Liq.*, 2012, **165**, 139–142.

36 R. F. C. Claridge, J. J. Kilpatrick and H. K. J. Powell, *Aust. J. Chem.*, 1980, **33**, 2757–2760.

37 The polymerized species of a similar structure ligand, 1,3-*N*,*N*,*N*′,*N*′-xylylenediamine tetraacetate copper(II) complex were synthesized and the structure was determined. Carboxylate oxygen atoms bridges copper(II) ions to form a 3D polymer. The structure will be published elsewhere.

38 (*a*) F. M. Al-Sogair, B. P. Operschall, A. Sigel, H. Sigel, J. Schnabl and R. K. O. Sigel, *Chem. Rev.*, 2011, **111**, 4964–5003; (*b*) L. E. Kapinos, B. P. Operschall, E. Larsen and H. Sigel, *Chem.–Eur. J.*, 2011, **17**, 8156–8164; (*c*) B. Knobloch, A. Mucha, B. P. Operschall, H. Sigel, M. Jezowska-Bojczuk, H. Kozlowski and R. K. O. Sigel, *Chem.–Eur. J.*, 2011, **17**, 5393–5403; (*d*) A. Sigel, B. P. Operschall and H. Sigel, *Coord. Chem. Rev.*, 2012, **256**, 260–278; (*e*) H. Sigel, B. P. Operschall and R. Griesser, *Chem. Soc. Rev.*, 2009, **38**, 2465–2494; (*f*) R. K. O. Sigel and H. Sigel, *Acc. Chem. Res.*, 2010, **43**, 974–984.

39 Y. Zhao, S. Zhu, M. Shao, T. Jia, M. Li, W. Lu and W. He, *Inorg. Chem. Commun.*, 2008, **11**, 925–928.

40 K. Mishra, H. Ojha and N. K. Chaudhury, *Food Chem.*, 2012, **130**, 1036–1043.

41 S.-I. Xiong, F. Lu, M.-J. Shi and Z.-M. Wu, *Shipin Gongye Keji*, 2012, **33**, 380–383.

42 R. A. Himes and K. D. Karlin, *Curr. Opin. Chem. Biol.*, 2009, **13**, 119–131.

43 M.-C.-I. Lee, Y. Kawai, H. Shoji, F. Yoshino, H. Miyazaki, H. Kato, M. Suga and E. Kubota, *Redox Rep.*, 2004, **9**, 331–336.

44 H. Yuzawa, M. Aoki, K. Otake, T. Hattori, H. Itoh and H. Yoshida, *J. Phys. Chem. C*, 2012, **116**, 25376–25387.

45 (*a*) S. Fukuzumi and K. D. Karlin, *Coord. Chem. Rev.*, 2013, **257**, 187–195; (*b*) S. Fukuzumi, L. Tahsini, Y.-M. Lee, K. Ohkubo, W. Nam and K. D. Karlin, *J. Am. Chem. Soc.*, 2012, **134**, 7025–7035.

46 (*a*) M. Katane and H. Homma, *Chem. Biodiversity*, 2010, **7**, 1435–1449; (*b*) Y. Li, O. Ogola Henry Joseph and Y. Sawa, *Appl. Microbiol. Biotechnol.*, 2011, **93**, 503–516; (*c*) L. Verrall, P. W. J. Burnet, J. F. Betts and P. J. Harrison, *Mol. Psychiatry*, 2009, **15**, 122–137.

47 B. Weiner, G. J. Poelarends, D. B. Janssen and B. L. Feringa, *Chem.–Eur. J.*, 2008, **14**, 10094–10100.

48 M. L. S. Cristiano, D. J. P. Gago, G. A. M. D. A. Rocha, R. A. W. Johnstone, M. McCarron and J. M. T. B. Varejao, *Org. Biomol. Chem.*, 2003, **1**, 565–574.

49 (*a*) K. Nomiya, K. Hashino, Y. Nemoto and M. Watanabe, *J. Mol. Catal. A: Chem.*, 2001, **176**, 79–86; (*b*) A. M. Khenkin, L. Weiner and R. Neumann, *J. Am. Chem. Soc.*, 2005, **127**, 9988–9989.

50 D. Bianchi, M. Bertoli, R. Tassinari, M. Ricci and R. Vignola, *J. Mol. Catal. A: Chem.*, 2003, **200**, 111–116.

51 K. Fujimoto, Y. Tokuda, H. Maekawa, Y. Matsubara, T. Mizuno and I. Nishiguchi, *Tetrahedron*, 1996, **52**, 3889–3896.

52 M. Makosza and K. Sienkiewicz, *J. Org. Chem.*, 1990, **55**, 4979–4981.

53 A. Fishman, Y. Tao, L. Rui and T. K. Wood, *J. Biol. Chem.*, 2005, **280**, 506–514.

54 J. C. D'Oliveira, C. Guillard, C. Maillard and P. Pichat, *J. Environ. Sci. Health, Part A*, 1993, **28**, 941–962.

55 G. Zhang and I. Hua, *Ind. Eng. Chem. Res.*, 2003, **42**, 285–289.

56 S. Kozuch and S. Shaik, *Acc. Chem. Res.*, 2011, **44**, 101–110.